

# Fluctuation Kinetics in a Multispecies Reaction-Diffusion System

Martin Howard

*Department of Physics, Theoretical Physics, University of Oxford, 1 Keble Road,  
Oxford, OX1 3NP, United Kingdom.*

## Abstract

We study fluctuation effects in a two species reaction-diffusion system, with three competing reactions  $A + A \rightarrow \emptyset$ ,  $B + B \rightarrow \emptyset$ , and  $A + B \rightarrow \emptyset$ . Asymptotic density decay rates are calculated for  $d \leq 2$  using two separate methods - the Smoluchowski approximation, and also field theoretic/renormalisation group (RG) techniques. Both approaches predict power law decays, with exponents which asymptotically depend only on the ratio of diffusion constants, and not on the reaction rates. Furthermore, we find that, for  $d < 2$ , the Smoluchowski approximation and the RG improved tree level give identical exponents. However, whereas the Smoluchowski approach cannot easily be improved, we show that the RG provides a systematic method for incorporating additional fluctuation effects. We demonstrate this advantage by evaluating one loop corrections for the exponents in  $d < 2$ , and find good agreement with simulations and exact results.

PACS Numbers: 02.50. -r, 05.40. +j, 82.20. -w.

# 1 Introduction

Over the past decade there has been enormous interest in reaction-diffusion systems (see [1–12] and references therein), with particular emphasis on the effects of fluctuations in low spatial dimensions. Most attention has been paid to reactions of the form  $A + A \rightarrow \emptyset$  and  $A + B \rightarrow \emptyset$  with a variety of different initial/boundary conditions. At or below an upper critical dimension  $d_c$ , these systems exhibit fluctuation induced anomalous kinetics, and the straightforward application of traditional approaches, such as mean field rate equations, breaks down. Attempts to understand the role played by fluctuations for  $d \leq d_c$  have involved several techniques, including Smoluchowski type approximations [9] and field theoretic methods [8, 10, 11]. In this paper we set out to study these fluctuation effects in a system with three competing reactions:



The reactions are irreversible, and we choose homogeneous, though not necessarily equal, initial densities for the two species at  $t = 0$ . Our goal is to calculate density decay exponents and amplitudes, taking into account fluctuation effects. In pursuit of this aim, we analyse the system using both the Smoluchowski approximation and the field theory approach, and we show that the two methods are closely related. However, whereas it is unclear how the Smoluchowski approach may be improved, the field theory provides a systematic way to obtain successively more accurate values for the asymptotic density decay exponents and amplitudes. We shall concentrate on situations where one of the two species is greatly in the majority (as is almost always the case asymptotically) - so, for example, if the A species is predominant, then we can safely neglect the reaction  $B + B \rightarrow \emptyset$ . This kind of assumption will lead to a considerable simplification in our analysis.

Previous work on this problem includes use of the Smoluchowski approximation

[9], as well as exact  $1d$  results obtained by Derrida *et al.* [15, 16, 17] for the special case of *immobile* minority particles. Derrida *et al.* were, in fact, studying a different problem, namely the probability that a given spin has never flipped in the zero temperature Glauber dynamics of the  $q$ -state Potts model in one dimension. By solving that model exactly [16, 17] they showed that this probability decreased as a power law:  $t^{-3/8}$  for the Ising ( $q = 2$ ) case. However, in one dimension, the Ising spin flip problem and the decay rate for the immobile impurity in our reaction-diffusion system are exactly equivalent problems, and hence this exact decay rate also holds in our case. We also mention one other previous result for the immobile impurity problem, due to Cardy [18]. Using renormalisation group methods similar to those employed in this paper, it was shown that the density of the minority species decays away as a universal power law:  $t^{-\beta}$  for  $d < 2$ , where  $\beta = \frac{1}{2} + O(\epsilon)$  and  $\epsilon = 2 - d$ .

The case where the *majority* species is immobile has also been solved (see [19]). In this case the decay rate for the minority species is dominated by minority impurity particles existing in regions where there happen to be very few of the majority particles. Since these majority particles are strictly stationary, this situation is not describable using a rate equation approach, and it turns out that the minority species decays away as  $\exp\left(-t^{d/(d+2)}\right)$ , a result which is not accessible by perturbative methods.

In this paper, using a field theory formalism and techniques from the renormalisation group, we will obtain decay rates and amplitudes for the general case of arbitrary diffusivities - a regime previously only accessible using the Smoluchowski approximation. Our basic plan is to map the microscopic dynamics, as described by a master equation, onto a quantum field theory. This theory is then renormalised (for  $d \leq 2$ ), and the couplings (reaction rates) are shown to have  $O(\epsilon)$  fixed points, whose values depend only on the ratio of the species' diffusion constants. Note

that this system (with irreversible reactions) is particularly simple in that only the couplings (and not the diffusivities) are renormalised. The next step is to group together Feynman diagrams which are of the same order in the renormalised couplings - i.e. diagrams with the same number of loops. These diagrams are then evaluated and a Callan-Symanzik equation used to obtain improved asymptotic  $\epsilon$  expansions for the densities. In this fashion, quantities of interest may be systematically calculated by successively including higher order sets of diagrams (with more loops) in the perturbative sum.

One consequence of the theory is that the asymptotic decay rates and amplitudes for  $d < d_c$  will be independent of the reaction rates - a result which is in accordance with the Smoluchowski approach. In fact, all physical quantities below the upper critical dimension asymptotically depend only on the diffusivities and the initial densities, and in this sense they display universality.

We now present a summary of our results for the density decay rates. In what follows we define  $n_A$ ,  $n_B$  to be the initial density of A, B particles, and  $\delta = (D_B/D_A) \leq 1$  to be the ratio of the diffusion constants. For  $d < d_c = 2$ ,  $n_A \gg n_B$  and  $n_A^{-2/d} D_A^{-1} \ll t \ll t_1$  (where  $t_1$  is a crossover time derived in section 4), we have (as in [8]):

$$\langle a \rangle \sim \left( \frac{1}{4\pi\epsilon} + \frac{2 \ln 8\pi - 5}{16\pi} + O(\epsilon) \right) (D_A t)^{-d/2}. \quad (1)$$

For the minority species, we find, from the RG improved tree level approximation in the field theory:

$$\langle b \rangle \sim F (D_A t)^{-\beta} \quad (2)$$

where

$$\beta \approx \frac{d}{2} \left( \frac{\delta + 1}{2} \right)^{d/2} \quad F \approx n_B \left( \frac{\Gamma(\epsilon/2)}{n_A (8\pi)^{d/2}} \right)^{\left( \frac{\delta+1}{2} \right)^{d/2}}. \quad (3)$$

These decay exponents are identical with the Smoluchowski results. Performing a strict  $\epsilon$  expansion on this RG improved tree level result gives an exponent  $\beta =$

$\frac{1}{2} + O(\epsilon)$  for the immobile impurity case ( $\delta = 0$ ). This is in agreement with previous RG calculations by Cardy [18]. If we now go beyond the tree level calculation by including one loop diagrams, then we obtain an improved value for the exponent  $\beta$  using an  $\epsilon$  expansion:

$$\beta = \left( \frac{1+\delta}{2} \right) \left( 1 - \frac{\epsilon}{2} \left[ \frac{3}{2} + \ln \left( \frac{1+\delta}{2} \right) - \frac{\delta(1+\delta)}{4} \left[ 1 + 2 \ln \left( \frac{1+\delta}{2} \right) \right] - \frac{1}{4}(\delta^2 - 1) \left( 1 + (1+\delta) \left[ f \left\{ \frac{2}{1+\delta} \right\} - \frac{\pi^2}{6} \right] \right) \right] \right) + O(\epsilon^2), \quad (4)$$

where

$$f\{x\} = - \int_1^x \frac{\ln u}{u-1} du \quad (5)$$

is the dilogarithmic function [20]. This exponent is found to be in good agreement with simulations [9] and exact results [16] in  $d = 1$ .

However, for  $\delta < 1$ , the system crosses over to a second regime where  $\langle b \rangle \gg \langle a \rangle$ . This situation is similar to the case where we begin with  $n_B \gg n_A$ . In that regime, at times  $D_B t \gg n_B^{-2/d}$ , and for  $n_B \gg n_A$ ,  $\delta \neq 0$  and  $d < 2$ , we have:

$$\langle b \rangle \sim \left( \frac{1}{4\pi\epsilon} + \frac{2 \ln 8\pi - 5}{16\pi} + O(\epsilon) \right) (D_B t)^{-d/2}, \quad (6)$$

for the majority species. Using the RG improved tree level result for the minority species, we obtain:

$$\langle a \rangle \sim E (D_B t)^{-\alpha}, \quad (7)$$

with

$$\alpha \approx \frac{d}{2} \left( \frac{1+\delta^{-1}}{2} \right)^{d/2} \quad E \approx n_A \left( \frac{\Gamma(\epsilon/2)}{n_B (8\pi)^{d/2}} \right)^{\left( \frac{1+\delta^{-1}}{2} \right)^{d/2}}. \quad (8)$$

The exponent is again in agreement with the Smoluchowski result. If we attempt to improve this calculation to one loop accuracy, then we obtain:

$$\alpha = \left( \frac{1+\delta^{-1}}{2} \right) \left( 1 - \frac{\epsilon}{2} \left[ \frac{3}{2} + \ln \left( \frac{1+\delta^{-1}}{2} \right) - \frac{\delta^{-1}(1+\delta^{-1})}{4} \left[ 1 + 2 \ln \left( \frac{1+\delta^{-1}}{2} \right) \right] - \frac{1}{4}(\delta^{-2} - 1) \left( 1 + (1+\delta^{-1}) \left[ f \left\{ \frac{2}{1+\delta^{-1}} \right\} - \frac{\pi^2}{6} \right] \right) \right] \right) + O(\epsilon^2). \quad (9)$$

This exponent is only valid for  $\delta$  quite close to unity, and even in this region it may be less accurate than the (non  $\epsilon$ -expanded) RG improved tree level result given above. This point will be discussed further in section 4.2.

We next give results valid for  $d = 2$ , where we find extra logarithmic factors multiplying the power law decay rates. Treating first the case  $\langle a \rangle \gg \langle b \rangle$  and  $\delta \leq 1$ , we have, from the RG improved tree level, an initial regime with:

$$\langle a \rangle \sim \frac{\ln t}{8\pi D_A t} \quad (10)$$

$$\langle b \rangle = O\left(\left(\frac{\ln t}{t}\right)^{\left(\frac{1+\delta}{2}\right)}\right). \quad (11)$$

However, for  $\delta < 1$ , the system again crosses over to a second regime where  $\langle b \rangle \gg \langle a \rangle$ . In this second regime the density decay exponents (though not the amplitudes) are the same as for the case where we begin with  $n_B \gg n_A$ . In that case we have, for  $\delta \neq 0$ :

$$\langle b \rangle \sim \frac{\ln t}{8\pi D_B t} \quad (12)$$

$$\langle a \rangle = O\left(\left(\frac{\ln t}{t}\right)^{\left(\frac{1+\delta^{-1}}{2}\right)}\right). \quad (13)$$

Crossover times for these cases are given in section 4.3.

We now give a brief description of the layout of this paper. In the next section we analyse the system using the mean field/Smoluchowski approach. We then set up the necessary formalism for our field theory in section 3, and use it to perturbatively calculate values for the density exponents and amplitudes in section 4. Finally, we give some conclusions and prospects for future work in section 5.

## 2 The Mean Field and Smoluchowski Approach

The simplest description of a reaction-diffusion process is provided by the mean field rate equations. For the system we are considering with densities  $a$  and  $b$ , they

take the form:

$$\frac{da}{dt} = -2\lambda_{AA}a^2 - \lambda_{AB}ab \quad (14)$$

$$\frac{db}{dt} = -2\lambda_{BB}b^2 - \lambda_{AB}ab, \quad (15)$$

where  $\lambda_{AA}$ ,  $\lambda_{BB}$ , and  $\lambda_{AB}$  are the reaction rates, and where we impose initial conditions of the form  $a|_{t=0} = n_A$  and  $b|_{t=0} = n_B$ . In this approach we have completely neglected the effects of fluctuations - in other words we have made assumptions of the form  $\langle ab \rangle \propto \langle a \rangle \langle b \rangle$  etc., where the angular brackets denote averages over the noise. Below the critical dimension, where fluctuations become relevant, this sort of approximation will break down.

Nevertheless, even at the mean field level, the complete solution set for these rate equations is quite complicated. In what follows we shall restrict our analysis to the case where  $2\lambda_{BB} < \lambda_{AB} < 2\lambda_{AA}$ . The solution for this particular parameter set will be required for our later field theoretic analysis. Following [9], it is easy to show (by forming a rate equation for the concentration ratio) that  $(a/b) \rightarrow 0$  as  $t \rightarrow \infty$ . Thus if we begin with initial conditions where  $n_A \gg n_B$ , we can identify two distinct regimes - an early time regime where  $a \gg b$  and, after a crossover, a late time (true asymptotic) regime where  $b \gg a$ . Treating the early time regime first, we find (after some algebra):

$$a \sim (2\lambda_{AA}t)^{-1} \quad (16)$$

$$b \sim \frac{n_B}{(2n_A\lambda_{AA}t)^{\lambda_{AB}/2\lambda_{AA}}}. \quad (17)$$

Note that the A particles are decaying away more quickly than the B's, so eventually we crossover to a second regime:

$$b \sim (2\lambda_{BB}t)^{-1} \quad (18)$$

$$a \sim \frac{n_A}{(2n_B\lambda_{BB}t)^{\lambda_{AB}/2\lambda_{BB}}} \left( 1 + \frac{(\lambda_{AB} - 2\lambda_{AA}) n_A}{(2\lambda_{BB} - \lambda_{AB}) n_B} \right)^{-1 - \frac{\lambda_{AB}(\lambda_{AB} - 2\lambda_{BB})}{2\lambda_{BB}(\lambda_{AB} - 2\lambda_{AA})}}. \quad (19)$$

Alternatively, if we begin with  $n_B \gg n_A$ , then we have a single asymptotic regime:

$$b \sim (2\lambda_{BB}t)^{-1} \quad (20)$$

$$a \sim \frac{n_A}{(2n_B\lambda_{BB}t)^{\lambda_{AB}/2\lambda_{BB}}}. \quad (21)$$

However, if we now wish to extend our results at or below the upper critical dimension, we must attempt to include some of the fluctuation effects. The simplest way in which this can be done is to employ the Smoluchowski approximation [13, 14, 9]. The essential idea of this approach is to relate the effective reaction rates  $\lambda_{\{ij\}}^{eff}$  to the diffusion constants  $D_A, D_B$ . Suppose we want to calculate the reaction rate  $\lambda_{AB}^{eff}$ . We begin by choosing a (fixed) A species target “trap”, which is surrounded by B particles. When a B particle approaches within a distance  $R$  of the target, a reaction is deemed to have occurred. Consequently, the reaction rate may be obtained by solving a diffusion equation with boundary conditions of fixed density as  $r \rightarrow \infty$ , and absorption at  $r = R$ . The flux of B particles across the  $d$  dimensional sphere of radius  $R$  is then proportional to an effective microscopic reaction rate. If we now generalise to the case where both the A and B species are mobile, then we find (in dimension  $d < 2$  and in the large time limit):

$$\lambda_{AB}^{eff} \sim (\text{const.})(D_A + D_B)^{d/2}t^{d/2-1}. \quad (22)$$

For  $d = 2$  we obtain logarithmic corrections:

$$\lambda_{AB}^{eff} \sim \frac{(\text{const.})(D_A + D_B)}{\ln((D_A + D_B)t)}. \quad (23)$$

The Smoluchowski reaction rates for  $\lambda_{AA}^{eff}$  and  $\lambda_{BB}^{eff}$  are obtained in a similar fashion. Note that above  $d = 2$  the reaction rate approaches a limiting (constant) value, and we see that the Smoluchowski approach predicts a critical dimension of  $d_c = 2$  for this system. This is simply related to the reentrancy property of random walks in  $d \leq 2$ . It is the inclusion of this effect which accounts for the improvement introduced by the Smoluchowski approach.

If we now substitute these modified reaction rates into the rate equations, we can obtain the Smoluchowski improved density exponents. For the case where  $n_A \gg n_B$ , we find an initial regime with

$$a = O(t^{-d/2}) \quad (24)$$

$$b = O\left(t^{-\frac{d}{2}\left(\frac{1+\delta}{2}\right)^{d/2}}\right). \quad (25)$$

Once again, since the A particles are decaying away faster than the B's, we cross over to a second regime, where (for  $0 < \delta < 1$ )

$$b = O(t^{-d/2}) \quad (26)$$

$$a = O\left(t^{-\frac{d}{2}\left(\frac{1+\delta^{-1}}{2}\right)^{d/2}}\right). \quad (27)$$

This second set of exponents is the same as for the case where we begin with  $n_B \gg n_A$  and  $\delta \neq 0$ . In this situation no crossover occurs and the exponents are valid for all asymptotic times. These exponents can be compared favourably with both simulations [9], and exact results [17]. For example, the decay rate for an immobile minority impurity is given by Smoluchowski to be  $\approx t^{-0.354}$ . This compares well with the exact decay rate of  $t^{-0.375}$ .

Turning to the case  $d = d_c = 2$  and  $n_A \gg n_B$ , we obtain, for the initial regime:

$$a = O\left(\frac{\ln t}{t}\right) \quad (28)$$

$$b = O\left(\left(\frac{\ln t}{t}\right)^{\left(\frac{1+\delta}{2}\right)} (\ln t)^{\left(\frac{1+\delta}{2}\right) \ln\left(\frac{1+\delta}{2}\right)}\right). \quad (29)$$

We again eventually crossover to a second regime, where (for  $0 < \delta < 1$ ):

$$b = O\left(\frac{\ln t}{t}\right) \quad (30)$$

$$a = O\left(\left(\frac{\ln t}{t}\right)^{\left(\frac{1+\delta^{-1}}{2}\right)} (\ln t)^{\left(\frac{1+\delta^{-1}}{2}\right) \ln\left(\frac{1+\delta^{-1}}{2}\right)}\right). \quad (31)$$

This second set of exponents is again valid (for all asymptotic times) in the case where we begin with  $n_B \gg n_A$  and  $\delta \neq 0$ .

Note that the Smoluchowski approach can also be employed for  $d > d_c$ , where again we will find (time independent) reaction rates which depend on the diffusion constants. However, in the general case, our later field theoretic analysis shows that there is no real justification for this procedure. One exception to this occurs in the case where we have heterogeneous single species annihilation, as considered in [9]. In this situation we have only one fundamental reaction process, but different reaction rates may still arise, for example, by having two or more different particle masses (and hence two or more different diffusion constants). In this case it is physically reasonable to suppose that the exponents (which are ratios of reaction rates) may depend only on the diffusivity ratios, with any other parameters canceling out. However, in the general case, where the reaction processes are genuinely distinct this will not be the case.

Overall, we have seen that the Smoluchowski approach is a simple way to incorporate some fluctuation effects into the rate equation approach. Unfortunately, it is not at all clear how these methods may be systematically improved. It is for this reason that we turn to the main purpose of this paper - the development of an alternative field theoretic framework.

### 3 The Field Theory Approach

Fluctuation effects in reaction-diffusion systems have previously been successfully tackled using techniques borrowed from quantum field theory and also from the renormalisation group. Examples include studies of the diffusion limited reactions  $A + A \rightarrow \emptyset$  [8] and  $A + B \rightarrow \emptyset$  [10, 11]. The first step in this analysis is to write down a Master Equation, which exactly describes the microscopic time evolution of the system. Using methods developed by Doi [21] and Peliti [22], this can be mapped onto a Schroedinger-like equation, with the introduction of a second

quantised Hamiltonian, and then onto a field theory, with an action  $S$ . These steps have been described in detail elsewhere [21, 22, 8, 10, 11], and consequently we shall simply give the resulting action appropriate for our theory:

$$S = \int d^d x \left( \int dt \left[ \bar{a}(\partial_t - \nabla^2)a + \bar{b}(\partial_t - \delta\nabla^2)b + 2\lambda_{AA}\bar{a}a^2 + \lambda_{AA}\bar{a}^2a^2 \right. \right. \\ \left. \left. + 2\lambda_{BB}\bar{b}b^2 + \lambda_{BB}\bar{b}^2b^2 + \lambda_{AB}\bar{a}ab + \lambda_{AB}\bar{b}ab + \lambda_{AB}\bar{a}\bar{b}ab \right] - \bar{a}n_A - \bar{b}n_B \right). \quad (32)$$

Here we have defined  $\delta = (D_B/D_A) \leq 1$  and also introduced the response fields  $\bar{a}$  and  $\bar{b}$ . In addition time  $t$ , together with the reaction rates  $\lambda_{\{ij\}}$  have been rescaled to absorb the diffusion constant  $D_A$ . Averaged quantities are then calculated according to

$$\langle X(t) \rangle = \mathcal{N}^{-1} \int \mathcal{D}a \mathcal{D}\bar{a} \mathcal{D}b \mathcal{D}\bar{b} X(t) e^{-S}, \quad (33)$$

where

$$\mathcal{N} = \int \mathcal{D}a \mathcal{D}\bar{a} \mathcal{D}b \mathcal{D}\bar{b} e^{-S}. \quad (34)$$

Notice that in the path integral

$$\int \mathcal{D}a \mathcal{D}\bar{a} \mathcal{D}b \mathcal{D}\bar{b} e^{-S} \quad (35)$$

integration over the fields  $\bar{a}$ ,  $a$  and  $\bar{b}$ ,  $b$  whilst neglecting the quartic terms, leads to a recovery of the mean field rate equations.

Performing power counting on the action  $S$ , we can now give the natural canonical dimensions for the various parameters appearing in the action:

$$[t] \sim k^{-2} \quad [a], [b], [n_A], [n_B] \sim k^d \quad [\bar{a}], [\bar{b}] \sim k^0 \quad [\lambda_{\{ij\}}] \sim k^{2-d}. \quad (36)$$

Notice that the reaction rates become dimensionless in  $d = 2$ , which we therefore postulate as the upper critical dimension for the system, in agreement with the Smoluchowski prediction.

From the action  $S$ , we can see that the propagators for the theory are given by

$$G_{a\bar{a}}(k, t - t') = \begin{cases} e^{-k^2(t-t')} & \text{for } t > t' \\ 0 & \text{for } t < t' \end{cases} \quad (37)$$

$$G_{b\bar{b}}(k, t - t') = \begin{cases} e^{-k^2(t-t')\delta} & \text{for } t > t' \\ 0 & \text{for } t < t'. \end{cases} \quad (38)$$

Diagrammatically, we represent  $G_{a\bar{a}}$  by a thin solid line and  $G_{b\bar{b}}$  by a thin dotted line. The vertices for the theory are given in figure 1.

### 3.1 Renormalisation

One of the most important features of this theory, as mentioned in the introduction, is the relative simplicity of its renormalisation. Examination of the vertices given in figure 1 reveals that it is not possible to draw diagrams which dress the propagators. Hence the bare propagators are the full propagators for the theory. Consequently, the only renormalisation needed involves the reaction rates  $\lambda_{\{ij\}}$ , and in particular the diffusion constants (or  $\delta$ ) are *not* renormalised.

The temporally extended vertex functions for the reaction rates are given by the diagrammatic sums given in figure 2. As is the case in similar theories [8, 10, 11], these sums may be evaluated exactly, using Laplace transforms:

$$\lambda_{AA}(k, s) = \frac{\lambda_{AA}}{1 + \lambda_{AA}C\Gamma(\epsilon/2)(s + \frac{1}{2}k^2)^{-\epsilon/2}} \quad (39)$$

$$\lambda_{BB}(k, s) = \frac{\lambda_{BB}}{1 + \lambda_{BB}C\Gamma(\epsilon/2)\delta^{-1}(s/\delta + \frac{1}{2}k^2)^{-\epsilon/2}} \quad (40)$$

$$\lambda_{AB}(k, s) = \frac{\lambda_{AB}}{1 + \lambda_{AB}2^{-\epsilon/2}C\Gamma(\epsilon/2)(1 + \delta)^{-d/2}(s + k^2\delta/(1 + \delta))^{-\epsilon/2}}, \quad (41)$$

where  $C = 2/(8\pi)^{d/2}$  and  $s$  is the Laplace transformed time variable.

We can now use these vertex functions to define the three dimensionless renormalised and bare couplings, with  $s = \kappa^2$ ,  $k = 0$  as the normalisation point:

$$g_{R_{\{ij\}}} = \kappa^{-\epsilon} \lambda_{\{ij\}}(k, s)|_{s=\kappa^2, k=0} \quad g_{0_{\{ij\}}} = \kappa^{-\epsilon} \lambda_{\{ij\}}. \quad (42)$$

Consequently, we can define three  $\beta$  functions:

$$\beta(g_{R_{AA}}) = \kappa \frac{\partial}{\partial \kappa} g_{R_{AA}} = -\epsilon g_{R_{AA}} + \epsilon C\Gamma(\epsilon/2) g_{R_{AA}}^2 \quad (43)$$

$$\beta(g_{R_{BB}}) = \kappa \frac{\partial}{\partial \kappa} g_{R_{BB}} = -\epsilon g_{R_{BB}} + \epsilon C\Gamma(\epsilon/2) \delta^{-d/2} g_{R_{BB}}^2 \quad (44)$$

$$\beta(g_{R_{AB}}) = \kappa \frac{\partial}{\partial \kappa} g_{R_{AB}} = -\epsilon g_{R_{AB}} + 2^{-\epsilon/2} \epsilon C\Gamma(\epsilon/2) (1 + \delta)^{-d/2} g_{R_{AB}}^2, \quad (45)$$

and three fixed points  $\beta(g_{R_{\{ij\}}^*}) = 0$ :

$$g_{R_{AA}}^* = (C\Gamma(\epsilon/2))^{-1} \quad (46)$$

$$g_{R_{BB}}^* = (C\Gamma(\epsilon/2) \delta^{-d/2})^{-1} \quad (47)$$

$$g_{R_{AB}}^* = \left( C\Gamma(\epsilon/2) \frac{1}{2} \left( \frac{1 + \delta}{2} \right)^{-d/2} \right)^{-1}. \quad (48)$$

Finally, we see from (39), (40), and (41) that the expansion of  $g_{0_{\{ij\}}}$  in powers of  $g_{R_{\{ij\}}}$  is given by:

$$g_{0_{\{ij\}}} = g_{R_{\{ij\}}} + \frac{g_{R_{\{ij\}}}^2}{g_{R_{\{ij\}}}^*} + \dots \quad (49)$$

### 3.2 Callan-Symanzik Equation

We now exploit the fact that physical quantities calculated using the field theory must be independent of the choice of normalisation point. This leads us to a Callan-Symanzik equation:

$$\left[ \kappa \frac{\partial}{\partial \kappa} + \beta(g_{R_{AA}}) \frac{\partial}{\partial g_{R_{AA}}} + \beta(g_{R_{BB}}) \frac{\partial}{\partial g_{R_{BB}}} + \beta(g_{R_{AB}}) \frac{\partial}{\partial g_{R_{AB}}} \right] \langle a \rangle_R = 0. \quad (50)$$

However dimensional analysis implies

$$\left[ \kappa \frac{\partial}{\partial \kappa} - 2t \frac{\partial}{\partial t} + dn_A \frac{\partial}{\partial n_A} + dn_B \frac{\partial}{\partial n_B} - d \right] \langle a \rangle_R(t, n_A, n_B, g_{R_{\{ij\}}}, \delta, \kappa) = 0. \quad (51)$$

Exactly similar equations hold for  $\langle b \rangle_R$ . Eliminating the terms involving  $\kappa$  and solving by the method of characteristics, we find:

$$\langle a \rangle_R(t, n_A, n_B, g_{R_{\{ij\}}}, \delta, \kappa) = (\kappa^2 t)^{-d/2} \langle a \rangle_R(\kappa^{-2}, \tilde{n}_A(\kappa^{-2}), \tilde{n}_B(\kappa^{-2}), \tilde{g}_{R_{\{ij\}}}(\kappa^{-2}), \delta, \kappa), \quad (52)$$

with the characteristic equations:

$$2t \frac{\partial \tilde{n}_A}{\partial t} = -d \tilde{n}_A \quad 2t \frac{\partial \tilde{n}_B}{\partial t} = -d \tilde{n}_B \quad 2t \frac{\partial \tilde{g}_{R_{\{ij\}}}}{\partial t} = \beta(\tilde{g}_{R_{\{ij\}}}), \quad (53)$$

and initial conditions:

$$\tilde{n}_A(t) = n_A \quad \tilde{n}_B(t) = n_B \quad (54)$$

$$\tilde{g}_{R_{AA}}(t) = g_{R_{AA}} \quad \tilde{g}_{R_{BB}}(t) = g_{R_{BB}} \quad \tilde{g}_{R_{AB}}(t) = g_{R_{AB}}. \quad (55)$$

These equations have the exact solutions:

$$\tilde{n}_A(t') = \left(\frac{t}{t'}\right)^{d/2} n_A \quad \tilde{n}_B(t') = \left(\frac{t}{t'}\right)^{d/2} n_B, \quad (56)$$

and

$$\tilde{g}_{R_{\{ij\}}}(t') = g_{R_{\{ij\}}}^* \left(1 + \frac{g_{R_{\{ij\}}}^* - g_{R_{\{ij\}}}}{g_{R_{\{ij\}}} (t/t')^{\epsilon/2}}\right)^{-1}. \quad (57)$$

In the large  $t$  limit  $\tilde{g}_{R_{\{ij\}}} \rightarrow g_{R_{\{ij\}}}^*$ , a relationship which will allow us to relate an expansion in powers of the renormalised couplings  $g_{R_{\{ij\}}}$  to an  $\epsilon$  expansion using (52). In our later density calculations we will assume that this asymptotic regime has been reached.

### 3.3 Tree Diagrams

In order to perform systematic  $\epsilon$  expansion calculations we now need to identify the leading and subleading terms in an expansion in powers of  $g_{0_{\{ij\}}}$ . In calculating  $\langle a \rangle$  and  $\langle b \rangle$ , contributions from tree diagrams are of order  $g_{0_{\{ij\}}}^q n_{\{i\}}^{1+q}$ , for integer  $q$ , and densities  $n_{\{i\}} = \{n_A, n_B\}$ . However, diagrams with  $l$  loops will be of order  $g_{0_{\{ij\}}}^{q+l} n_{\{i\}}^{1+q}$ . The addition of loops makes the power  $g_{0_{\{ij\}}}$  higher relative to the power of the densities - so we conclude that the number of loops gives the order of the diagram.

The lowest order diagrams contributing to  $\langle a \rangle$  and  $\langle b \rangle$  are the tree diagrams shown in figure 3. We represent the classical (tree level) density  $\langle a \rangle_{cl}$  by a wavy solid line, and  $\langle b \rangle_{cl}$  by a wavy dotted line. These sets of diagrams are equivalent to the mean field rate equations, as may be seen by acting on each by their respective inverse Green functions.

The second tree level quantities appearing in the theory are the response functions:

$$L(k, t_2, t_1) = \langle a(-k, t_2) \bar{a}(k, t_1) \rangle \quad (58)$$

$$M(k, t_2, t_1) = \langle b(-k, t_2) \bar{a}(k, t_1) \rangle \quad (59)$$

$$N(k, t_2, t_1) = \langle b(-k, t_2) \bar{b}(k, t_1) \rangle \quad (60)$$

$$P(k, t_2, t_1) = \langle a(-k, t_2) \bar{b}(k, t_1) \rangle \quad (61)$$

which we represent diagrammatically by the thick lines shown in figure 4. These functions can be evaluated analytically, but only in the limit  $\langle a \rangle \gg \langle b \rangle$ , or  $\langle b \rangle \gg \langle a \rangle$ . The details of this calculation are presented in appendix A, where the following results are derived (for  $\langle a \rangle \gg \langle b \rangle$ ):

$$L(k, t_2, t_1) = \left( \frac{1 + 2\lambda_{AA}n_A t_1}{1 + 2\lambda_{AA}n_A t_2} \right)^2 \exp(-k^2(t_2 - t_1)) \quad (62)$$

$$N(k, t_2, t_1) = \left( \frac{1 + 2\lambda_{AA}n_A t_1}{1 + 2\lambda_{AA}n_A t_2} \right)^{\lambda_{AB}/2\lambda_{AA}} \exp(-k^2(t_2 - t_1)\delta) \quad (63)$$

$$P(k, t_2, t_1) = -\lambda_{AB}n_A \frac{(1 + 2\lambda_{AA}n_A t_1)^{\lambda_{AB}/2\lambda_{AA}}}{(1 + 2\lambda_{AA}n_A t_2)^2} \exp(-k^2(t_2 - t_1)\delta) \\ \times \int_{t_1}^{t_2} \frac{\exp(k^2(1 - \delta)t')}{(1 + 2\lambda_{AA}n_A t')^{-1 + \lambda_{AB}/2\lambda_{AA}}} dt' \quad (64)$$

$$M(k, t_2, t_1) = -\lambda_{AB}n_B \frac{(1 + 2\lambda_{AA}n_A t_1)^2}{(1 + 2\lambda_{AA}n_A t_2)^{\lambda_{AB}/2\lambda_{AA}}} \exp(-k^2(t_2\delta - t_1)) \\ \times \int_{t_1}^{t_2} \frac{\exp(-k^2(1 - \delta)t')}{(1 + 2\lambda_{AA}n_A t')^2} dt'. \quad (65)$$

An extra check on validity of these response functions is provided by the relations:

$$L(0, t, 0) = \frac{\partial \langle a(t) \rangle}{\partial n_A} \quad N(0, t, 0) = \frac{\partial \langle b(t) \rangle}{\partial n_B} \quad (66)$$

$$P(0, t, 0) = \frac{\partial \langle a(t) \rangle}{\partial n_B} \quad M(0, t, 0) = \frac{\partial \langle b(t) \rangle}{\partial n_A}, \quad (67)$$

which follow from the definition of the response functions, and from the initial condition terms in the action  $S$ . It is easy to check that the above response functions do indeed satisfy these relations.

For the opposite situation where  $n_B \gg n_A$  (and hence  $\langle b \rangle \gg \langle a \rangle$ ), we could use a formalism similar to the above for the density calculations. However, it is much simpler to map this case onto the  $\langle a \rangle \gg \langle b \rangle$  regime by swapping the labels on the A and B particles, and then relabeling:

$$n_A \leftrightarrow n_B \quad \lambda_{AA} \leftrightarrow \lambda_{BB} \quad D_A \leftrightarrow D_B.$$

We can then obtain the exponents and amplitudes for this second regime with no extra work.

This concludes our discussion of the field theory formalism. The framework we have built up allows (in principle) the systematic calculation of fluctuation effects in all circumstances. However, it is only in the case where one of the species is greatly in the majority where the equations (for the tree level densities and response functions) are sufficiently simple for analytic progress to be made. We now turn to use of the field theory in calculating the fluctuation modified densities.

## 4 Density Calculations

### 4.1 Tree Level

The first step in using our field theory to include fluctuation effects is to insert the mean field (tree level) solution into the Callan-Symanzik solution (52), using the results for the running densities/couplings (56), (57). Since the fixed points for the couplings obey  $2g_{R_{BB}}^* < g_{R_{AB}}^* < 2g_{R_{AA}}^*$  (when  $\delta < 1$ ) it is appropriate to use the mean field solutions derived in section 2. For the case where  $n_A \gg n_B$ , this gives:

$$\langle a \rangle \sim \left( \frac{\Gamma(\epsilon/2)}{(8\pi)^{d/2}} \right) (D_A t)^{-d/2}, \quad (68)$$

and

$$\langle b \rangle \sim F(D_A t)^{-\beta}, \quad (69)$$

with

$$\beta \approx \frac{d}{2} \left( \frac{1+\delta}{2} \right)^{d/2} \quad F \approx n_B \left( \frac{\Gamma(\epsilon/2)}{n_A (8\pi)^{d/2}} \right)^{\left(\frac{1+\delta}{2}\right)^{d/2}}, \quad (70)$$

valid for  $n_A^{-2/d} D_A^{-1} \ll t \ll t_1$ , where

$$D_A t_1 \approx \left( \frac{n_B}{n_A \left(\frac{1+\delta}{2}\right)^{d/2}} \right)^{\frac{2}{d} \left( \left(\frac{1+\delta}{2}\right)^{d/2} - 1 \right)^{-1}}. \quad (71)$$

These modified crossover times are obtained by using the expressions for the running couplings/densities in the mean field crossovers. Notice that the density decay exponents derived here are the same as those obtained from the Smoluchowski approach. However, as we are performing an  $\epsilon$  expansion, we are only strictly justified in retaining leading order  $\epsilon$  terms. Consequently we find, for the minority species density decay exponent and amplitude:

$$\beta = \left( \frac{1+\delta}{2} \right) + O(\epsilon) \quad F = n_B \left( \frac{1}{4\pi\epsilon n_A} + O(\epsilon^0) \right)^{\left(\frac{1+\delta}{2}\right) + O(\epsilon)}. \quad (72)$$

Eventually, however, as the A particles are decaying away more quickly than the B particles (due to their greater diffusivity when  $\delta < 1$ ), we crossover to a second regime where  $\langle b \rangle \gg \langle a \rangle$ . For  $0 < \delta < 1$ , we have:

$$\langle b \rangle \sim \left( \frac{\Gamma(\epsilon/2)}{(8\pi)^{d/2}} \right) (D_B t)^{-d/2} \quad (73)$$

$$\langle a \rangle \sim E (D_B t)^{-\alpha}, \quad (74)$$

with

$$\alpha \approx \frac{d}{2} \left( \frac{1+\delta^{-1}}{2} \right)^{d/2} = \left( \frac{1+\delta^{-1}}{2} \right) + O(\epsilon) \quad (75)$$

$$E \approx n_A f(d) \left( \frac{\Gamma(\epsilon/2)}{n_B (8\pi)^{d/2}} \right)^{\left(\frac{1+\delta^{-1}}{2}\right)^{d/2}} = n_A f(2) \left( \frac{1}{4\pi\epsilon n_B} + O(\epsilon^0) \right)^{\left(\frac{1+\delta^{-1}}{2}\right) + O(\epsilon)} \quad (76)$$

where

$$f(d) = \left( 1 + \frac{[\left(\frac{(1+\delta)/2}{\delta^{d/2}} - 1\right) n_A]}{[\delta^{d/2} - \left(\frac{(1+\delta)/2}{\delta^{d/2}}\right) n_B]} \right)^{-1 - \left(\frac{1+\delta^{-1}}{2}\right)^{d/2} \left( \frac{\left(\frac{(1+\delta)/2}{\delta^{d/2}} - \delta^{d/2}\right)}{\left(\frac{(1+\delta)/2}{\delta^{d/2}} - 1\right)} \right)}. \quad (77)$$

This result is valid for  $t \gg t_2$ , where

$$D_B t_2 \approx \left( \frac{n_A f(d) (1 + \delta^{-1})^{d/2}}{n_B^{((1+\delta^{-1})/2)^{d/2}}} \right)^{\frac{2}{d}} \left( \left( \frac{1+\delta^{-1}}{2} \right)^{d/2} - 1 \right)^{-1}. \quad (78)$$

Note that for  $\delta = 1$  the first crossover time  $t_1 \rightarrow \infty$  - in this case the two species decay away at the same rate, and so no further crossover occurs. Alternatively if  $\delta = 0$ , then the first regime is left, but the second crossover time  $t_2 \rightarrow \infty$ . In that case the minority species finally decays away in the exponential fashion predicted in [19]. For the intermediate case where  $\delta$  is small, but nonzero, the decay exponent for the minority species becomes large in the final regime. The explanation for this result lies in the relatively large diffusivity of the minority A species (if  $D_A$  is large) and/or the increased density amplitude for the majority B particles (if  $D_B$  is small). Both these effects will lead to an increased rate of decay for the A species.

Finally, if the initial conditions are changed such that now  $n_B \gg n_A$ , with  $\delta \neq 0$ , then we obtain the same results as for the second of the above regimes for  $D_B t \gg n_B^{-2/d}$ , with  $f \approx 1$ .

## 4.2 One Loop Results

We now describe the one loop improvements to the tree level result. In the regime  $\langle a \rangle \gg \langle b \rangle$ , the dominant diagrams will be those where the minimum possible number of  $\langle b \rangle_{cl}$  insertions are made. For the majority A species the appropriate diagram is shown in figure 5, where there are no  $\langle b \rangle_{cl}$  insertions. This is identical to the one loop diagram for  $A + A \rightarrow \emptyset$  evaluated in [8], which gives, in conjunction with the subleading terms from the tree level:

$$\langle a \rangle \sim \left( \frac{1}{4\pi\epsilon} + \frac{2 \ln 8\pi - 5}{16\pi} + O(\epsilon) \right) (D_A t)^{-d/2}. \quad (79)$$

In addition, for that subset of diagrams with no  $\langle b \rangle_{cl}$  insertions, the decay exponent is exact. More details of this calculation, including a demonstration of the

cancellation of divergences, can be found in [8].

Turning now to the one loop calculation for the minority species, the appropriate diagrams are the three shown in figure 6, each of which contains just one  $\langle b \rangle_{cl}$  insertion:

$$(i) \quad \frac{-4\lambda_{AB}\lambda_{AA}^2 n_A^2 n_B}{(2\lambda_{AA} n_A t)^{1+\lambda_{AB}/2\lambda_{AA}}} \int \frac{d^d k}{(2\pi)^d} \int_0^t dt_2 \int_0^{t_2} dt_1 (t - t_2) \times \frac{(1 + 2\lambda_{AA} n_A t_1)^2}{(1 + 2\lambda_{AA} n_A t_2)^3} \exp[-2k^2(t_2 - t_1)] \quad (80)$$

$$(ii) \quad \frac{-2\lambda_{AB}^2 \lambda_{AA} n_A^2 n_B}{(2\lambda_{AA} n_A t)^{\lambda_{AB}/2\lambda_{AA}}} \int \frac{d^d k}{(2\pi)^d} \int_0^t dt_2 \int_0^{t_2} dt_1 \int_{t_1}^{t_2} dt' \frac{(1 + 2\lambda_{AA} n_A t_1)^2}{(1 + 2\lambda_{AA} n_A t_2)^2} \times \frac{1}{(1 + 2\lambda_{AA} n_A t')^2} \exp[-k^2(t_2(1 + \delta) - 2t_1 + (1 - \delta)t')] \quad (81)$$

$$(iii) \quad \frac{\lambda_{AB}^2 n_A n_B}{(2\lambda_{AA} n_A t)^{\lambda_{AB}/2\lambda_{AA}}} \int \frac{d^d k}{(2\pi)^d} \int_0^t dt_2 \int_0^{t_2} dt_1 \frac{(1 + 2\lambda_{AA} n_A t_1)}{(1 + 2\lambda_{AA} n_A t_2)^2} \times \exp[-k^2(1 + \delta)(t_2 - t_1)]. \quad (82)$$

The detail of the evaluation of these diagrams is rather subtle. Essentially we are interested in extracting the most divergent parts of these integrals, which will turn out to be pieces of  $O(\epsilon^{-1})$  and  $O(\epsilon^0)$ . However, we must be careful not to confuse genuine bare divergences (of  $O(\epsilon^{-1})$  which must be removed by the renormalisation of the theory), with logarithmic pieces, which we must retain. The divergences arise in diagrams (i) and (iii) as the difference in time  $t_2 - t_1$  between the beginning and end of the loops tends to zero (in  $d = 2$ ). After the process of renormalisation we find corrections of the form:

$$1 + (\text{constant})\epsilon \ln((\text{constant})t^{d/2}) + O(\epsilon^2). \quad (83)$$

If this series is identified as the expansion of an exponential, then we find that our one loop diagrams (together with subleading components from the tree level) have provided  $O(\epsilon)$  corrections to the exponents.

Diagrams (i) and (iii) are relatively straightforward to evaluate. The  $k$  and  $t_1$  integrals are elementary, and the final  $t_2$  integrals can be done by parts to extract

the necessary most divergent pieces (up to  $O(\epsilon^0)$ ). The second diagram of figure 6 is more complicated, and we perform its evaluation in appendix B - although we are only able to extract the logarithmic piece of  $O(t^{-\lambda_{AB}/2\lambda_{AA}} t^{\epsilon/2} \ln t)$ . There will be corrections to this of  $O(t^{-\lambda_{AB}/2\lambda_{AA}} t^{\epsilon/2})$  (contributing to a modified amplitude) which we have been unable to calculate. We find asymptotically:

$$(i) \frac{-\lambda_{AB}n_B}{8\pi(2\lambda_{AA}n_At)^{\lambda_{AB}/2\lambda_{AA}}} \left( \frac{2t^{\epsilon/2}(\ln(2\lambda_{AA}n_At) - 1)}{\epsilon} + t^{\epsilon/2}(\ln(2\lambda_{AA}n_At) - 1) \ln(8\pi) \right. \\ \left. + \frac{15t^{\epsilon/2}}{4} - \frac{3}{2}t^{\epsilon/2} \ln(2\lambda_{AA}n_At) - \int_0^t t_2^{-1+\epsilon/2} \ln(1 + 2\lambda_{AA}n_At_2) dt_2 + O(\epsilon) \right) \quad (84)$$

$$(ii) \frac{-\lambda_{AB}^2 n_B}{32\pi\lambda_{AA}(2\lambda_{AA}n_At)^{\lambda_{AB}/2\lambda_{AA}}} \left( \delta + \frac{1}{2}(\delta^2 - 1) \left[ \ln \left( \frac{1 - \delta}{1 + \delta} \right) \right. \right. \\ \left. \left. - \int_{-1}^{\frac{1-\delta}{1+\delta}} dv \frac{(1+v)^2}{v^2} \ln(1+v) \right] + O(\epsilon) \right) t^{\epsilon/2} \ln(2\lambda_{AA}n_At) \quad (85)$$

$$(iii) \frac{\lambda_{AB}^2 n_B (4\pi(1 + \delta))^{-1}}{2\lambda_{AA}(2\lambda_{AA}n_At)^{\lambda_{AB}/2\lambda_{AA}}} \left( \frac{2t^{\epsilon/2} \ln(2\lambda_{AA}n_At)}{\epsilon} + t^{\epsilon/2} \ln(2\lambda_{AA}n_At) \ln(4\pi(1 + \delta)) \right. \\ \left. - t^{\epsilon/2}(\ln(2\lambda_{AA}n_At) - 1) - \int_0^t t_2^{-1+\epsilon/2} \ln(1 + 2\lambda_{AA}n_At_2) dt_2 + O(\epsilon) \right). \quad (86)$$

To one loop accuracy we can make the replacement:  $\lambda_{\{ij\}} = \kappa^\epsilon g_{0\{ij\}} \rightarrow \kappa^\epsilon g_{R\{ij\}}$ .

These results must now be combined with the subleading terms from the tree level.

Using (49), we find

$$\langle b \rangle \sim \frac{n_B}{(2\lambda_{AA}n_At)^{\lambda_{AB}/2\lambda_{AA}}} = \frac{n_B}{(2\kappa^\epsilon g_{R_{AA}} n_At)^{g_{R_{AB}}/2g_{R_{AA}}}} \left( 1 - \frac{g_{R_{AB}}}{2g_{R_{AA}}^*} \right. \\ \left. - \frac{g_{R_{AB}}^2}{2g_{R_{AA}} g_{R_{AB}}^*} \ln(2\kappa^\epsilon g_{R_{AA}} n_At) + \frac{g_{R_{AB}}}{2g_{R_{AA}}^*} \ln(2\kappa^\epsilon g_{R_{AA}} n_At) + O(g_R^2) \right). \quad (87)$$

If we now insert explicit  $\epsilon$  expanded values for the fixed points  $g_{R\{ij\}}^*$ , then we discover that the bare divergences cancel between (84), (86), and (87). With insertion into the Callan-Symanzik solution (52), we also find that the pieces we have left as integrals in (i) and (iii) (which are  $O(t^{\epsilon/2}(\ln t)^2)$ ) also mutually cancel. Eventually we find:

$$\langle b \rangle \sim (\text{const.}) t^{-\frac{d}{2}(\frac{1+\delta}{2})^{d/2}} \left( 1 + \frac{\epsilon(1 + \delta)}{8} \left[ 1 - 2(1 + \delta) \left( \frac{\delta}{4} + \frac{\delta^2 - 1}{8} \left( \ln \left( \frac{1 - \delta}{1 + \delta} \right) \right) \right) \right] \right)$$

$$- \int_{-1}^{\frac{1-\delta}{1+\delta}} dv \frac{(1+v)^2 \ln(1+v)}{v^2} \Big) \Big] \ln((\text{const.})t^{d/2}) + O(\epsilon^2) \Big), \quad (88)$$

where we have neglected  $O(\epsilon)$  pieces which, aside from the prefactor, are time *independent*. These terms contribute only to the density amplitude. We now evaluate the integral in (88), using

$$\begin{aligned} \int_{-1}^{\frac{1-\delta}{1+\delta}} \frac{\ln(1+v)}{v} dv &= \int_0^{\frac{2}{1+\delta}} \frac{\ln u}{u-1} du = \int_0^1 \frac{\ln u}{u-1} du + \int_1^{\frac{2}{1+\delta}} \frac{\ln u}{u-1} du \\ &= \frac{\pi^2}{6} - f\left\{\frac{2}{1+\delta}\right\}, \end{aligned} \quad (89)$$

where  $f\{x\}$  is the dilogarithm function [20]. The other parts of the integral are elementary. The next step is to  $\epsilon$  expand the RG improved tree level result:

$$\frac{d}{2} \left( \frac{1+\delta}{2} \right)^{d/2} = \left( \frac{1+\delta}{2} \right) \left( 1 - \frac{\epsilon}{2} \left( 1 + \ln \left( \frac{1+\delta}{2} \right) \right) + O(\epsilon^2) \right). \quad (90)$$

Then, exponentiating the  $\epsilon$  expansion in (88), we find  $\langle b \rangle = O(t^{-\beta})$ , where

$$\begin{aligned} \beta &= \left( \frac{1+\delta}{2} \right) \left( 1 - \frac{\epsilon}{2} \left[ \frac{3}{2} + \ln \left( \frac{1+\delta}{2} \right) - \frac{\delta(1+\delta)}{4} \left[ 1 + 2 \ln \left( \frac{1+\delta}{2} \right) \right] \right. \right. \\ &\quad \left. \left. - \frac{1}{4}(\delta^2 - 1) \left( 1 + (1+\delta) \left[ f\left\{\frac{2}{1+\delta}\right\} - \frac{\pi^2}{6} \right] \right) \right] \right) + O(\epsilon^2). \end{aligned} \quad (91)$$

$\beta$  is plotted as a function of  $\delta$  for  $\epsilon = 1$  ( $d = 1$ ) in figure 9. For the case where  $\delta = 1$ , we recover the decay rate  $\langle b \rangle = O(t^{-d/2})$ . This is to be expected, as when  $\delta = 1$  we are effectively again dealing with a single species reaction-diffusion system (at least for  $d < 2$ ). In that case the density decay exponent is known to all orders in perturbation theory [8], and is in agreement with our result. For the case where  $\delta = 0$  and  $d = 1$ , the decay exponent is also known exactly to be  $\langle b \rangle = O(t^{-0.375})$  [17]. This can be compared with our result, where we find

$$\beta = \frac{1}{16} + \frac{1}{4} \ln 2 + \frac{\pi^2}{64} \approx 0.39 \quad (\delta = 0). \quad (92)$$

Consequently, this answer is a modest improvement over the Smoluchowski result derived in section 2, and also in [9].

For the case  $n_B \gg n_A$  (and hence  $\langle b \rangle \gg \langle a \rangle$ ), we could follow the same route as described above, by evaluating the one loop diagrams shown in figures 7 and 8. However, as we mentioned in the last section we can much more easily obtain these corrections by swapping the labels on the A and B particles, and then relabeling:

$$n_A \leftrightarrow n_B \quad \lambda_{AA} \leftrightarrow \lambda_{BB} \quad D_A \leftrightarrow D_B.$$

Following this procedure, the majority species amplitude/exponent can be found by taking  $D_A \rightarrow D_B$  in equation (79):

$$\langle b \rangle \sim \left( \frac{1}{4\pi\epsilon} + \frac{2 \ln 8\pi - 5}{16\pi} + O(\epsilon) \right) (D_B t)^{-d/2}. \quad (93)$$

We can obtain the one loop minority species exponent by substituting  $\delta \rightarrow \delta^{-1}$  in equation (91):

$$\langle a \rangle = O(t^{-\alpha}), \quad (94)$$

where

$$\begin{aligned} \alpha = & \left( \frac{1 + \delta^{-1}}{2} \right) \left( 1 - \frac{\epsilon}{2} \left[ \frac{3}{2} + \ln \left( \frac{1 + \delta^{-1}}{2} \right) - \frac{\delta^{-1}(1 + \delta^{-1})}{4} \left[ 1 + 2 \ln \left( \frac{1 + \delta^{-1}}{2} \right) \right] \right. \right. \\ & \left. \left. - \frac{1}{4}(\delta^{-2} - 1) \left( 1 + (1 + \delta^{-1}) \left[ f \left\{ \frac{2}{1 + \delta^{-1}} \right\} - \frac{\pi^2}{6} \right] \right) \right] \right) + O(\epsilon^2). \quad (95) \end{aligned}$$

Notice, however, that in forming the one loop corrections for the minority species exponent, we have had to expand the RG improved tree level result:

$$\frac{d}{2} \left( \frac{1 + \delta^{-1}}{2} \right)^{d/2} = \left( \frac{1 + \delta^{-1}}{2} \right) \left( 1 - \frac{\epsilon}{2} \left( 1 + \ln \left( \frac{1 + \delta^{-1}}{2} \right) \right) + O(\epsilon^2) \right). \quad (96)$$

The error arising from this expansion will become large as  $\delta$  becomes small. Eventually this inaccuracy will cause the exponent to reach a maximum and then *decrease* as  $\delta$  is further reduced - behaviour which is clearly unphysical. In order to reduce the error, and to ensure that the expansion in equation (96) is qualitatively correct, we need to retain the  $O(\epsilon^2)$  terms. Hence the one loop exponent in equation (95) should be treated with some caution - terms of order  $O(\epsilon^2)$  will probably be

required for precise results. Consequently the (non  $\epsilon$  expanded) RG improved tree level result given in the last section may be more accurate in this regime. In figure 10 we have plotted the one loop exponent  $\alpha$  as a function of  $\delta$ , for  $d = 1$  ( $\epsilon = 1$ ), in the region  $0.7 \leq \delta \leq 1$ , where the exponent is still *increasing* for decreasing  $\delta$ .

In principle, calculations can also be made for the case with  $n_A \gg n_B$ , but where we have crossed over to the regime  $\langle b \rangle \gg \langle a \rangle$  (for  $0 < \delta < 1$  and times  $t \gg t_2$ ). However, a rigorous evaluation of the one loop diagrams is now much more difficult, as the functional forms for the densities and response functions will change over time. Nevertheless, since the above corrections to the exponents come from asymptotic logarithmic terms, it is plausible to suppose that the new exponent corrections will be dominated by contributions from the final asymptotic regime. If this is indeed the case, then the one loop exponents (though *not* the amplitudes) will be unchanged from the previous results (equations (93) to (95)). This calculation will, however, suffer from the same problem as described above.

### 4.3 $d = d_c$

For the case  $d = d_c = 2$  we expect logarithmic corrections to the decay exponents, as the reaction rates  $\lambda_{\{ij\}}$  are marginal parameters at the critical dimension. We can find the running couplings from the characteristic equation (53) by taking the limit  $\epsilon \rightarrow 0$  in equations (43), (44), and (45):

$$\tilde{g}_{R_{AA}}(\kappa^{-2}) = \frac{g_{R_{AA}}}{1 + g_{R_{AA}} C \ln(\kappa^2 t)} \sim (C \ln t)^{-1} \quad (97)$$

$$\tilde{g}_{R_{BB}}(\kappa^{-2}) = \frac{g_{R_{BB}}}{1 + g_{R_{BB}} C \delta^{-1} \ln(\kappa^2 t)} \sim (C \delta^{-1} \ln t)^{-1} \quad (98)$$

$$\tilde{g}_{R_{AB}}(\kappa^{-2}) = \frac{g_{R_{AB}}}{1 + g_{R_{AB}} C (1 + \delta)^{-1} \ln(\kappa^2 t)} \sim (C (1 + \delta)^{-1} \ln t)^{-1}, \quad (99)$$

where we have taken the asymptotic limits. Corrections to the asymptotic running couplings will be an order  $(\ln t)^{-1}$  smaller, and consequently these asymptotic

expressions will only be correct at very large times. Hence our expressions for the densities will only be valid when both this condition, and the crossover time constraints given below, are satisfied. In what follows we shall assume the validity of the first of these two conditions. Notice that the asymptotic running couplings are still ordered  $2\tilde{g}_{R_{BB}} < \tilde{g}_{R_{AB}} < 2\tilde{g}_{R_{AA}}$  for  $\delta < 1$ , so we can use the mean field solutions derived in section 2 as the basis for the RG improved tree level exponents and amplitudes. Making use of the Callan-Symanzik solution (52) and the above running couplings, we find for  $\langle a \rangle \gg \langle b \rangle$ :

$$\langle a \rangle \sim \frac{\ln t}{8\pi D_A t} \quad (100)$$

$$\langle b \rangle \sim \frac{n_B}{(8\pi n_A G D_A t / \ln t)^{(1+\delta)/2}}, \quad (101)$$

where  $G = \exp\left(\frac{4\pi}{g_{R_{AA}}}\left(1 - \frac{(1+\delta)g_{R_{AA}}}{g_{R_{AB}}}\right)\right)$  is a non-universal amplitude correction. Note that the next order terms for the minority species are suppressed by a factor of only  $(\ln \ln t)/(\ln t)$ . Using our expressions for the running couplings/densities in the mean field crossovers, we find that these expressions are valid for times  $D_A^{-1} n_A^{-1} \ln t \ll t \ll T_1$ , where

$$(D_A T_1 / \ln T_1) \approx \left(\frac{(G n_A)^{(1+\delta)/2}}{n_B}\right)^{\frac{2}{1-\delta}}. \quad (102)$$

For the case  $\delta < 1$  the system will eventually enter a second regime, where now the B species will be in the majority. We have (for  $\delta \neq 0$ ):

$$\langle b \rangle \sim \frac{\ln t}{8\pi D_B t} \quad (103)$$

$$\langle a \rangle \sim \frac{n_A K}{(8\pi n_B H D_B t / \ln t)^{(1+\delta^{-1})/2}}, \quad (104)$$

with

$$H = \exp\left(\frac{4\pi\delta}{g_{R_{BB}}}\left(1 - \frac{(1+\delta^{-1})g_{R_{BB}}}{g_{R_{AB}}}\right)\right) \quad K = \left(1 + \frac{n_A}{n_B}\right)^{\frac{\delta^{-1}-1}{2}}. \quad (105)$$

This is valid for times when  $t \gg T_2$ , where

$$(D_B T_2 / \ln T_2) \approx \left(\frac{(H n_B)^{(1+\delta^{-1})/2}}{n_A (1+\delta^{-1}) K}\right)^{\frac{2}{1-\delta^{-1}}}. \quad (106)$$

Alternatively, if we begin with  $n_B \gg n_A$ , then for  $\delta \neq 0$  and  $(D_B t / \ln t) \gg n_B^{-1}$ , we have the same results as for the second of the above cases, with  $K \approx 1$ . Interestingly, the logarithmic corrections we have derived in this section using the RG approach differ slightly from the Smoluchowski results given in section 2.

## 5 Conclusion

In this paper we have made a comparison of two methods for treating fluctuation effects in a reaction-diffusion system. We have found that the Smoluchowski and field theory approaches are rather similar - the Smoluchowski approximation, for  $d < 2$ , giving the same exponents as the renormalisation group improved tree level in the field theory. In addition, we have gone on to calculate the field theoretic one loop corrections, which have yielded improved values for the exponents. The advantage of the field theory is that it provides a systematic way to calculate these corrections - a procedure which is lacking in the Smoluchowski approach. Furthermore the use of renormalisation group techniques has demonstrated universality in the asymptotic amplitudes and exponents, in that, for  $d < 2$ , they only depend on the diffusivities and the initial densities, and not on the reaction rates.

The theory we have developed in this paper can easily be extended to slightly different situations. Consider first an annihilation/coagulation reaction-diffusion system, where the following reactions occur:



The Smoluchowski approach differs from before only in the absence of factors of 2 in the rate equation terms describing the same species reactions. Consequently, if we begin with  $n_A \gg n_B$  then the minority species will decay as

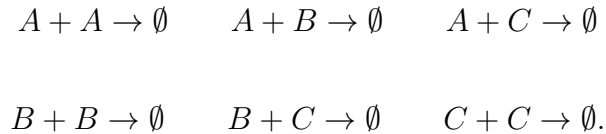
$$b = O\left(t^{-d\left(\frac{1+\delta}{2}\right)^{d/2}}\right) \quad (d < 2). \quad (107)$$

On the other hand, the field theory description lacks only the factors of 2 in the action (32). If this difference is followed through then the decay exponent in the RG improved tree level is seen to be the same as in the Smoluchowski approach. However, this difference of a factor of 2 has a major effect on the response functions (where this factor appears as a power), and as a result the new one loop corrections will be different from those calculated in section 4.2. These results should be compared with the exact solution [23, 24, 25] for the minority species decay rate  $b = O(t^{-\gamma})$ , where:

$$\gamma = \frac{\pi}{2 \cos^{-1}(\delta/(1 + \delta))}. \quad (108)$$

Note that in this case, although the Smoluchowski answer is qualitatively correct, it deviates considerably from the exact answer. Hence we can see that application of the Smoluchowski approach does not always lead to accurate exponents.

Another possible extension is to consider reaction-diffusion systems with more than two species of particle. For example, examining a three species system, we could have the reactions:



Analysis of this situation is very similar to before, and we merely remark that in the appropriate asymptotic regimes the Smoluchowski and RG improved tree level exponents (consisting of ratios of diffusion constants) are once again identical. Hence the convergence between the Smoluchowski exponents and those obtained from the RG improved tree level is fairly robust, and is not simply confined to the two species systems we have previously been considering. A further possibility is to analyse the case where we have a continuous distribution of diffusivities, but with only a *single* reaction channel. This has been studied from the Smoluchowski

point of view by Krapivsky *et al.* [9], and it would be interesting to extend our RG methods to include this situation.

Our theory could also be employed to consider clustered immobile reactants - a generalisation of the  $\delta = 0$  case included in our calculations. This situation has been analysed by Ben-Naim [12], using the Smoluchowski approach, where the dimension of the cluster  $d_I$  was found to substantially affect the kinetics. Specifically, for codimensionality  $d - d_I < 2$  (in a space of dimension  $d$ ) a finite fraction of the impurities was found to survive, whereas for  $d - d_I \geq 2$  the clusters decayed away indefinitely. The formalism we have presented in this paper could be adapted to study this clustered impurity problem, where calculations could be made without reliance on the Smoluchowski approach.

**Acknowledgments.** The author thanks John Cardy for suggesting this problem and for many useful discussions. Financial support from the EPSRC is also acknowledged.

## 6 Appendix A: Response Functions

Obtaining an exact analytic expression for the response functions is, in general, very hard. Suppose we define the “trunk” to be the line of propagators onto which the density lines are attached, as shown at the bottom of figure 4. Difficulties arise from diagrams where the “trunk” changes from one propagator into the other, and then back again, as shown in last of the diagrams for the  $L$  response function in figure 4. If diagrams of this type are initially excluded then progress can be made. Consider first the two subseries shown in figure 11, for the functions  $\xi(k, t_2, t_1)$  and  $\theta(k, t_2, t_1)$ , where diagrams of the above kind have been excluded. These series can

be summed exactly (using the same technique as described in [8]), giving:

$$\xi(k, t_2, t_1) = \exp(-k^2(t_2 - t_1)) \exp\left(-\int_{t_1}^{t_2} (4\lambda_{AA}a + \lambda_{AB}b)dt\right) \quad (109)$$

$$\theta(k, t_2, t_1) = \exp(-k^2(t_2 - t_1)\delta) \exp\left(-\int_{t_1}^{t_2} (4\lambda_{BB}b + \lambda_{AB}a)dt\right). \quad (110)$$

The full response functions are now given by the diagrammatic equations shown in figure 12, where all possible diagrams are included. Written out explicitly these give:

$$L(k, t_2, t_1) = \xi(k, t_2, t_1) - \lambda_{AB} \int_{t_1}^{t_2} \xi(k, t_2, \tau) a(\tau) M(k, \tau, t_1) d\tau \quad (111)$$

$$M(k, t_2, t_1) = -\lambda_{AB} \int_{t_1}^{t_2} \theta(k, t_2, \tau) b(\tau) L(k, \tau, t_1) d\tau \quad (112)$$

$$N(k, t_2, t_1) = \theta(k, t_2, t_1) - \lambda_{AB} \int_{t_1}^{t_2} \theta(k, t_2, \tau) b(\tau) P(k, \tau, t_1) d\tau \quad (113)$$

$$P(k, t_2, t_1) = -\lambda_{AB} \int_{t_1}^{t_2} \xi(k, t_2, \tau) a(\tau) N(k, \tau, t_1) d\tau. \quad (114)$$

In general this set of coupled integral equations is intractable - however we can make progress in the limit where  $\langle a \rangle \gg \langle b \rangle$ , or  $\langle b \rangle \gg \langle a \rangle$ . Considering the case where  $\langle a \rangle \gg \langle b \rangle$ , the dominant contributions to the response functions come from diagrams with the minimum possible number of  $\langle b \rangle_{cl}$  density line insertions. Accordingly, we can now truncate the full diagrammatic equations, as shown in figure 13. Notice that to this order  $L$ ,  $N$ , and  $P$  contain no  $\langle b \rangle_{cl}$  density insertions, whereas  $M$  must contain one such insertion. In this approximation we can now perform the integrals inside the  $\xi$  and  $\theta$  functions, using the appropriate mean field density:

$$\int_{t_1}^{t_2} (4\lambda_{AA}a + \lambda_{AB}b)dt \approx \int_{t_1}^{t_2} \frac{4\lambda_{AA}n_A}{1 + 2\lambda_{AA}n_A t} dt = \ln \left( \frac{1 + 2\lambda_{AA}n_A t_2}{1 + 2\lambda_{AA}n_A t_1} \right)^2 \quad (115)$$

$$\int_{t_1}^{t_2} (4\lambda_{BB}b + \lambda_{AB}a)dt \approx \int_{t_1}^{t_2} \frac{\lambda_{AB}n_A}{1 + 2\lambda_{AA}n_A t} dt = \ln \left( \frac{1 + 2\lambda_{AA}n_A t_2}{1 + 2\lambda_{AA}n_A t_1} \right)^{\lambda_{AB}/2\lambda_{AA}}, \quad (116)$$

and therefore

$$\xi(k, t_2, t_1) = \left( \frac{1 + 2\lambda_{AA}n_A t_1}{1 + 2\lambda_{AA}n_A t_2} \right)^2 \exp(-k^2(t_2 - t_1)) \quad (117)$$

$$\theta(k, t_2, t_1) = \left( \frac{1 + 2\lambda_{AA}n_A t_1}{1 + 2\lambda_{AA}n_A t_2} \right)^{\lambda_{AB}/2\lambda_{AA}} \exp(-k^2(t_2 - t_1)\delta). \quad (118)$$

Using these expressions, it is now straightforward to derive the response functions given in equations (62), (63), (64), and (65).

## 7 Appendix B: A One Loop Integral

For the case where  $\langle a \rangle \gg \langle b \rangle$  the hardest of the three diagrams of figure 6 to evaluate is (ii) - see equation (81). We shall evaluate it first in  $d = 2$ , and then deduce its form in  $d = 2 - \epsilon$ . Notice that the extra integration resulting from the  $\langle b \rangle_d$  insertion in the loop ensures that this diagram is not divergent. Taking the asymptotic part of the  $t_1$  and  $t'$  pieces, we find:

$$\begin{aligned} & \frac{-\lambda_{AB}^2 n_B}{2\lambda_{AA}(2\lambda_{AA}n_A t)^{\lambda_{AB}/2\lambda_{AA}}} \int \frac{d^2 k}{(2\pi)^2} \int_0^t dt_2 \int_0^{t_2} dt_1 \int_{t_1}^{t_2} dt' \frac{(2\lambda_{AA}n_A)^2 t_1^2}{(1 + 2\lambda_{AA}n_A t_2)^2 t'^2} \\ & \times \exp(-k^2(t_2(1 + \delta) - 2t_1 + (1 - \delta)t')). \end{aligned} \quad (119)$$

The  $k$  and  $t'$  integrals are elementary, giving

$$\begin{aligned} & \frac{-\lambda_{AB}^2 n_B}{8\pi\lambda_{AA}(2\lambda_{AA}n_A t)^{\lambda_{AB}/2\lambda_{AA}}} \int_0^t \frac{dt_2 (2\lambda_{AA}n_A)^2}{(1 + 2\lambda_{AA}n_A t_2)^2} \int_0^{t_2} dt_1 t_1^2 \\ & \times \left( \frac{1}{(t_2(1 + \delta) - 2t_1)} \left[ \frac{1}{t_1} - \frac{1}{t_2} \right] + \frac{1 - \delta}{(t_2(1 + \delta) - 2t_1)^2} \ln \left( \frac{2t_1}{(1 + \delta)t_2} \right) \right). \end{aligned} \quad (120)$$

Although the first part of the  $t_1$  integral is straightforward, the second piece involving the logarithm is more difficult. However, if we make the transformation

$$v = \frac{2t_1}{(1 + \delta)t_2} - 1, \quad (121)$$

we find:

$$\int_0^{t_2} dt_1 \frac{(1-\delta)t_1^2}{(t_2(1+\delta)-2t_1)^2} \ln\left(\frac{2t_1}{(1+\delta)t_2}\right) = \frac{1}{8}(1-\delta^2)t_2 \int_{-1}^{\frac{1-\delta}{1+\delta}} dv \frac{(1+v)^2}{v^2} \ln(1+v), \quad (122)$$

where all time dependency has been removed from the integral limits. The final  $t_2$  integral is then easy to perform, and we end up with:

$$\begin{aligned} & \frac{-\lambda_{AB}^2 n_B}{32\pi\lambda_{AA}(2\lambda_{AA}n_{At})^{\lambda_{AB}/2\lambda_{AA}}} \left( \delta + \frac{1}{2}(\delta^2 - 1) \left[ \ln\left(\frac{1-\delta}{1+\delta}\right) \right. \right. \\ & \left. \left. - \int_{-1}^{\frac{1-\delta}{1+\delta}} dv \frac{(1+v)^2}{v^2} \ln(1+v) \right] \right) \ln(2\lambda_{AA}n_{At}). \end{aligned} \quad (123)$$

However, we now need to extend this analysis to determine the behaviour of the integral in  $d = 2 - \epsilon$ . If we take the asymptotic part of all the pieces inside the integral, and perform power counting, we find that it should scale as  $t^{-\lambda_{AB}/2\lambda_{AA}} t^{\epsilon/2}$ . However, this procedure is not strictly valid, as in moving to the asymptotic version a false  $t_2 = 0$  divergence is created. Nevertheless, the integral is dominated by contributions from late times where arguments based on power counting should be valid. Hence in  $d = 2 - \epsilon$  we find:

$$\begin{aligned} & \frac{-\lambda_{AB}^2 n_B}{32\pi\lambda_{AA}(2\lambda_{AA}n_{At})^{\lambda_{AB}/2\lambda_{AA}}} \left( \delta + \frac{1}{2}(\delta^2 - 1) \left[ \ln\left(\frac{1-\delta}{1+\delta}\right) \right. \right. \\ & \left. \left. - \int_{-1}^{\frac{1-\delta}{1+\delta}} dv \frac{(1+v)^2}{v^2} \ln(1+v) \right] + O(\epsilon) \right) t^{\epsilon/2} \ln(2\lambda_{AA}n_{At}). \end{aligned} \quad (124)$$

Further subleading corrections (in time), which we have not calculated, will lack the logarithm factor, and so will contribute to the *amplitude* for the minority species density.

## References

- [1] Toussaint D and Wilczek F 1983 *J. Chem. Phys.* **78** 2642
- [2] Kang K and Redner S 1985 *Phys. Rev. A* **32** 435
- [3] Kuzovkov V and Kotomin E 1988 *Rep. Prog. Phys.* **51** 1479
- [4] Gálfi L and Rácz Z 1988 *Phys. Rev. A* **38** 3151
- [5] Ovchinnikov A, Timashev S and Belyy A 1990 *Kinetics of Diffusion Controlled Chemical Processes* (New York: Nova Science Publishers)
- [6] Ben-Naim E and Redner S 1992 *J. Phys. A: Math. Gen.* **25** L575
- [7] Cornell S and Droz M 1993 *Phys. Rev. Lett.* **70** 3824
- [8] Lee B 1994 *J. Phys. A: Math. Gen.* **27** 2633
- [9] Krapivsky P, Ben-Naim E and Redner S 1994 *Phys. Rev. E* **50** 2474
- [10] Lee B and Cardy J 1995 *J. Stat. Phys.* **80** 971
- [11] Howard M and Cardy J 1995 *J. Phys. A: Math. Gen.* **28** 3599
- [12] Ben-Naim E 1994 *Preprint cond-mat 9412048*
- [13] Smoluchowski M 1917 *Z. Phys. Chem.* **92** 215
- [14] Chandrasekhar S 1943 *Rev. Mod. Phys.* **15** 1
- [15] Derrida B, Bray A and Godrèche C 1994 *J. Phys. A: Math. Gen.* **27** L357
- [16] Derrida B 1995 *J. Phys. A: Math. Gen.* **28** 1481
- [17] Derrida B, Hakim V and Pasquier V 1995 *Phys. Rev. Lett.* **75** 751
- [18] Cardy J 1995 *J. Phys. A: Math. Gen.* **28** L19

- [19] Grassberger P and Procaccia I 1982 *J. Chem. Phys.* **77** 6281
- [20] Abramowitz M and Stegun I 1965 *Handbook of Mathematical Functions* (New York: Dover)
- [21] Doi M 1976 *J. Phys. A: Math. Gen.* **9** 1465, 1479
- [22] Peliti L 1985 *J. Physique* **46** 1469
- [23] Fisher M E 1984 *J. Stat. Phys.* **34** 667
- [24] Fisher M E and Gelfand M P 1988 *J. Stat. Phys.* **53** 175
- [25] ben-Avraham D 1988 *J. Chem. Phys.* **88** 941

## List of Figures

1	Vertices for the field theory. . . . .	34
2	The temporally extended vertex functions (a) $\lambda_{AA}(k, s)$ , (b) $\lambda_{BB}(k, s)$ , and (c) $\lambda_{AB}(k, s)$ . . . . .	34
3	Tree level diagrams for the densities $\langle a \rangle$ and $\langle b \rangle$ . . . . .	35
4	The response functions. . . . .	35
5	One loop diagram for $\langle a \rangle$ (when $\langle a \rangle \gg \langle b \rangle$ ). . . . .	36
6	One loop diagrams for $\langle b \rangle$ (when $\langle a \rangle \gg \langle b \rangle$ ). . . . .	36
7	One loop diagram for $\langle b \rangle$ (when $\langle b \rangle \gg \langle a \rangle$ ). . . . .	36
8	One loop diagrams for $\langle a \rangle$ (when $\langle b \rangle \gg \langle a \rangle$ ). . . . .	37
9	The one loop density decay exponent $\beta$ for the minority B species ( $\langle b \rangle = O(t^{-\beta})$ ) as a function of $\delta$ . . . . .	38
10	The one loop density decay exponent $\alpha$ for the minority A species ( $\langle a \rangle = O(t^{-\alpha})$ ) as a function of $\delta$ (for $0.7 \leq \delta \leq 1$ ). . . . .	39
11	The diagrammatic equations for (a) $\xi$ and (b) $\theta$ . . . . .	40
12	The full diagrammatic equations satisfied by the response functions. . . . .	40
13	The truncated diagrammatic equations for the response functions, valid for $\langle a \rangle \gg \langle b \rangle$ , or $\langle b \rangle \gg \langle a \rangle$ . . . . .	41

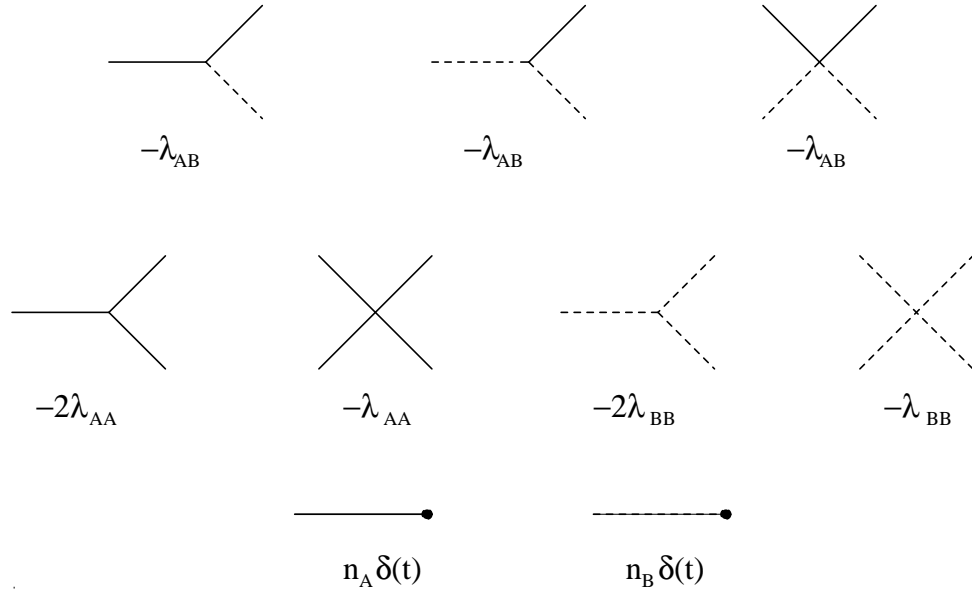


Figure 1: Vertices for the field theory.

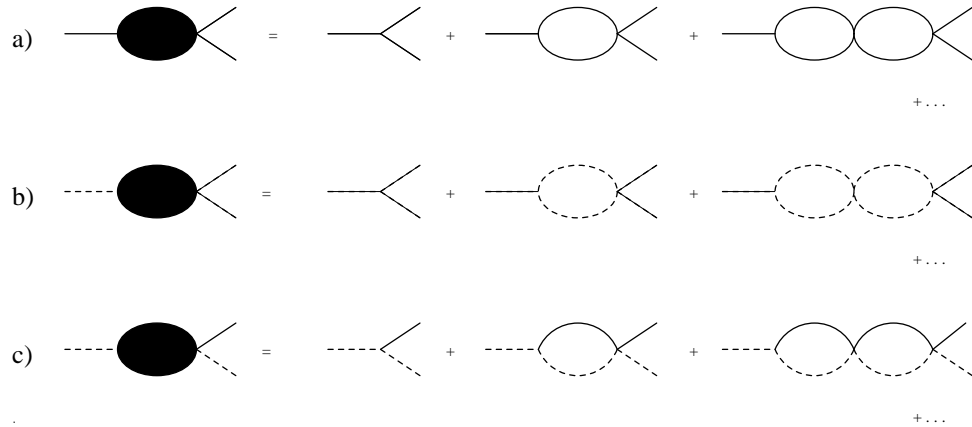


Figure 2: The temporally extended vertex functions (a)  $\lambda_{AA}(k, s)$ , (b)  $\lambda_{BB}(k, s)$ , and (c)  $\lambda_{AB}(k, s)$ .

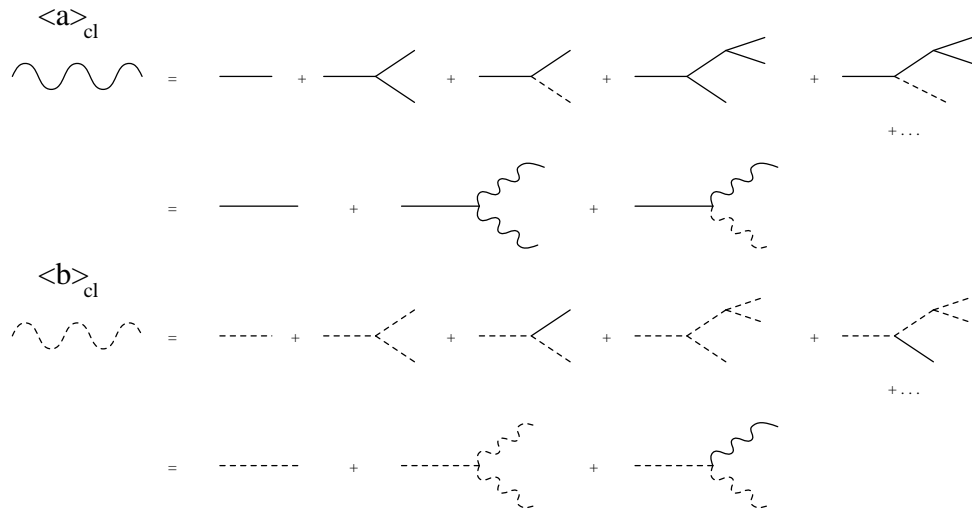
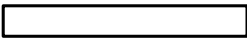


Figure 3: Tree level diagrams for the densities  $\langle a \rangle$  and  $\langle b \rangle$ .

$L =$  

$P =$  

$M =$  

$N =$  

where, for example :

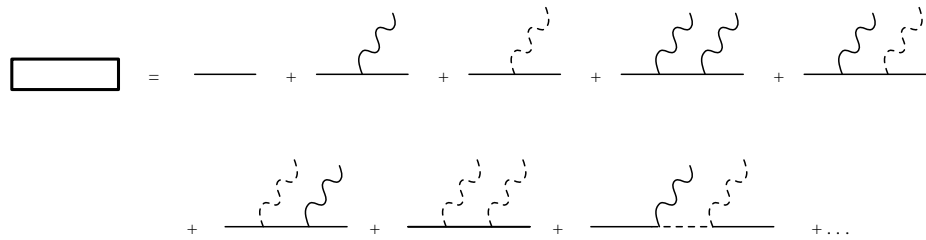


Figure 4: The response functions.

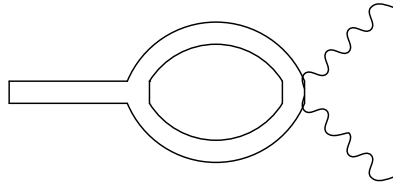


Figure 5: One loop diagram for  $\langle a \rangle$  (when  $\langle a \rangle \gg \langle b \rangle$ ).

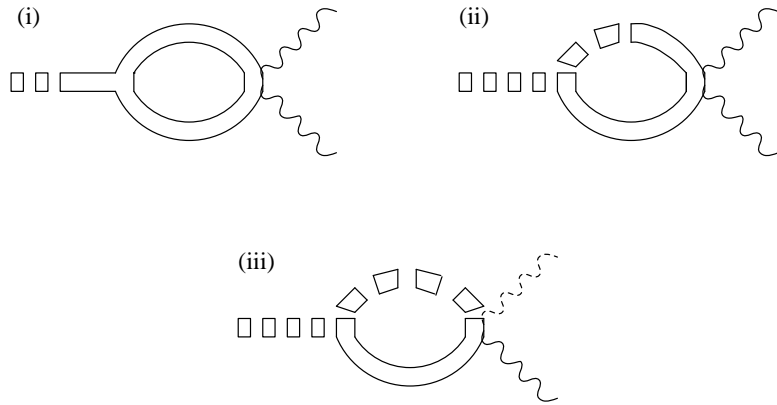


Figure 6: One loop diagrams for  $\langle b \rangle$  (when  $\langle a \rangle \gg \langle b \rangle$ ).

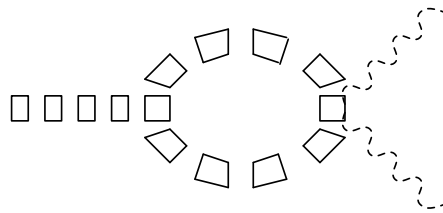


Figure 7: One loop diagram for  $\langle b \rangle$  (when  $\langle b \rangle \gg \langle a \rangle$ ).

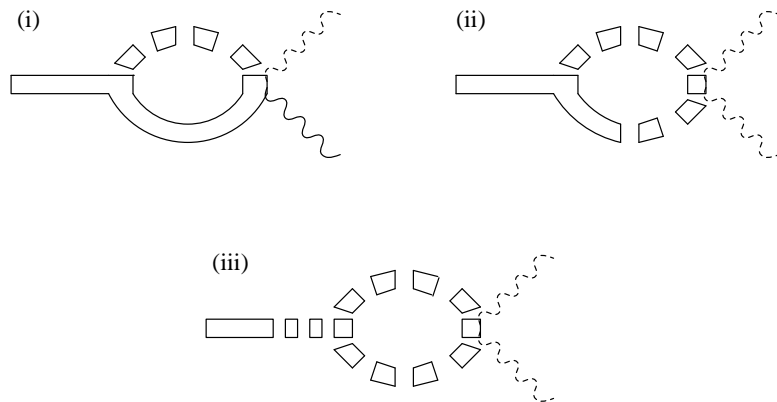


Figure 8: One loop diagrams for  $\langle a \rangle$  (when  $\langle b \rangle \gg \langle a \rangle$ ).

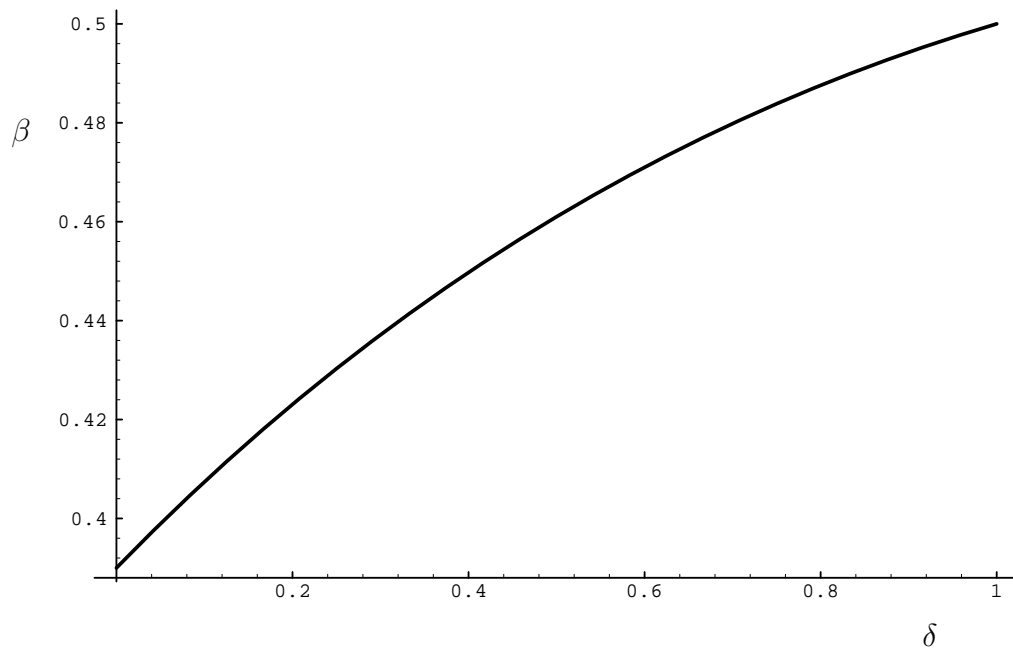


Figure 9: The one loop density decay exponent  $\beta$  for the minority B species ( $\langle b \rangle = O(t^{-\beta})$ ) as a function of  $\delta$ .

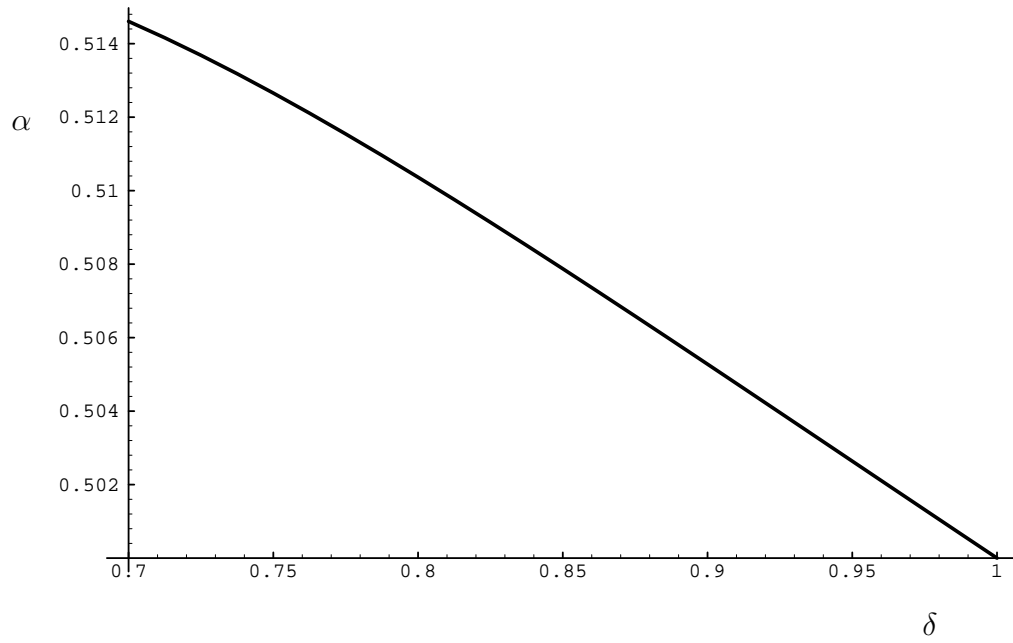
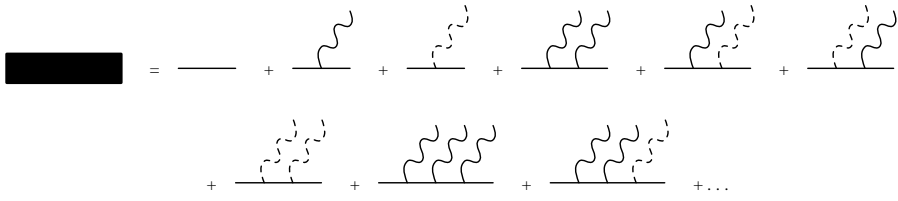
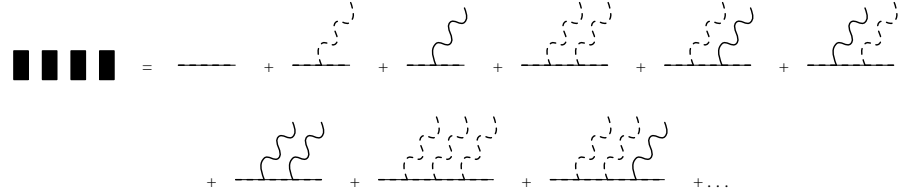


Figure 10: The one loop density decay exponent  $\alpha$  for the minority A species ( $\langle a \rangle = O(t^{-\alpha})$ ) as a function of  $\delta$  (for  $0.7 \leq \delta \leq 1$ ).

a) 

$$\blacksquare = \text{---} + \text{---} \begin{array}{l} \text{wavy} \\ \text{line} \end{array} + \text{---} \begin{array}{l} \text{dashed} \\ \text{line} \end{array} + \text{---} \begin{array}{l} \text{wavy} \\ \text{loop} \end{array} + \text{---} \begin{array}{l} \text{wavy} \\ \text{line} \\ \text{dashed} \\ \text{line} \end{array} + \text{---} \begin{array}{l} \text{wavy} \\ \text{line} \\ \text{dashed} \\ \text{line} \\ \text{wavy} \\ \text{line} \end{array} + \dots$$

b) 

$$\blacksquare \blacksquare \blacksquare \blacksquare = \text{---} + \text{---} \begin{array}{l} \text{dashed} \\ \text{line} \end{array} + \text{---} \begin{array}{l} \text{wavy} \\ \text{line} \end{array} + \text{---} \begin{array}{l} \text{dashed} \\ \text{line} \\ \text{dashed} \\ \text{line} \end{array} + \text{---} \begin{array}{l} \text{dashed} \\ \text{line} \\ \text{wavy} \\ \text{line} \end{array} + \text{---} \begin{array}{l} \text{dashed} \\ \text{line} \\ \text{wavy} \\ \text{line} \\ \text{dashed} \\ \text{line} \end{array} + \dots$$

Figure 11: The diagrammatic equations for (a)  $\xi$  and (b)  $\theta$ .



$$\square = \blacksquare + \blacksquare \begin{array}{l} \text{wavy} \\ \text{line} \end{array} + \blacksquare \begin{array}{l} \text{dashed} \\ \text{line} \end{array} + \blacksquare \begin{array}{l} \text{wavy} \\ \text{line} \\ \text{dashed} \\ \text{line} \end{array} + \blacksquare \begin{array}{l} \text{wavy} \\ \text{line} \\ \text{dashed} \\ \text{line} \\ \text{wavy} \\ \text{line} \end{array} + \dots$$

$$\square = \blacksquare + \blacksquare \begin{array}{l} \text{wavy} \\ \text{line} \end{array} \square \square \square$$

$$\square \square = \blacksquare \begin{array}{l} \text{wavy} \\ \text{line} \end{array} \blacksquare \blacksquare \blacksquare + \blacksquare \begin{array}{l} \text{wavy} \\ \text{line} \\ \text{dashed} \\ \text{line} \end{array} \blacksquare \blacksquare \blacksquare + \dots$$

$$\square \square = \blacksquare \begin{array}{l} \text{wavy} \\ \text{line} \end{array} \square \square \square$$

$$\square \square \square = \blacksquare \blacksquare \blacksquare + \blacksquare \blacksquare \blacksquare \begin{array}{l} \text{dashed} \\ \text{line} \end{array} \blacksquare \blacksquare \blacksquare + \blacksquare \blacksquare \blacksquare \begin{array}{l} \text{dashed} \\ \text{line} \\ \text{wavy} \\ \text{line} \end{array} \blacksquare \blacksquare \blacksquare + \blacksquare \blacksquare \blacksquare \begin{array}{l} \text{dashed} \\ \text{line} \\ \text{wavy} \\ \text{line} \\ \text{dashed} \\ \text{line} \end{array} \blacksquare \blacksquare \blacksquare + \dots$$

$$\square \square \square = \blacksquare \blacksquare \blacksquare + \blacksquare \blacksquare \blacksquare \begin{array}{l} \text{dashed} \\ \text{line} \end{array} \square \square$$

Figure 12: The full diagrammatic equations satisfied by the response functions.

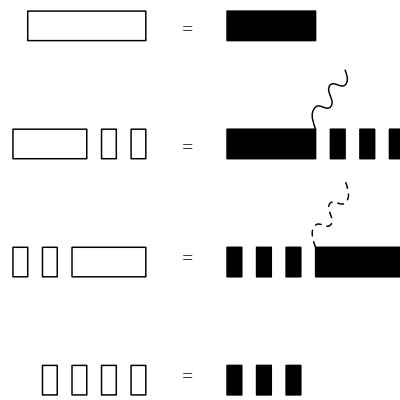


Figure 13: The truncated diagrammatic equations for the response functions, valid for  $\langle a \rangle \gg \langle b \rangle$ , or  $\langle b \rangle \gg \langle a \rangle$ .